CEAI, Vol.22, No.2 pp. 3-12, 2020 Printed in Romania

Petri-Net based Modelling and Multi-Objective Optimal Deployment for WRSN

Huaiyu Qin*, **, Leijun Xu*,
Buhui Zhao*, Jun Wan***

**School of Electrical and Information Engineering, Jiangsu University, Zhenjiang 212000, P R China*
China (Tel: 0086-511-88791240; e-mail: xlking@ujs.edu.cn, zhaobuhui@ujs.edu.cn)
*** Jiangsu University of Science and Technology, Zhenjiang 212000, P R China*
China (e-mail: qhy@just.edu.cn)
****Changzhou University, Changzhou 213000, P R China*
China (e-mail: qiaosan@sina.com)

Abstract: Fixed Charger Deployment (FCD) is a key issue for Wireless Rechargeable Sensor Network (WRSN). Since both the cost and network utility should be taken into account, the optimization of the chargers' number, transmitting power, and deployment location is particularly important. Accordingly, the FCD is formulated as a multi-objective optimization problem, where the objectives are to minimize the transmitting power of chargers and maximize the received power of sensor nodes. To quantitatively and visually describe the deployment, the Generalized Synchronizing Colored Cyber Petri Nets (GSCCPN) is presented to model the FCD. A Charger Deployment Multi-Objective Genetic Algorithm (CDMOGA) based on NSGA2 has been proposed. Simulation results show that the proposed algorithm can optimize both the charging power and the network utility, having a better performance than the algorithms of MOEA/D and SPEA2.

Keywords: Wireless rechargeable sensor networks, Petri-nets, Charging deployment, Multi-objective optimization, Genetic algorithm.

1. INTRODUCTION

Wireless sensor networks have been widely used in many applications including transportation, fire warning, wildlife protection and intrusion detection etc. Sensors are deployed in parking lots to guide drivers to vacant parking spaces quickly (Wei et al., 2017). Sensors are placed in the forest for fire early warning and soil erosion monitoring (Lloret et al., 2009). Sensors are utilized to track the activities of rare species (Dominguez-Morales et al., 2016). Sensors are deployed in the military region to detect intrusion attacks (Alqahtani et al., 2019). However, the limited battery energy of sensor nodes will greatly shorten the life of wireless sensor network and bring high maintenance cost. The wireless sensor network with energy harvesting came into being. Wireless Rechargeable Sensor Network (WRSN) is a typical representative. The main challenge in WRSN is how to deploy the fixed chargers. Though many pioneering works dedicated on deployment optimization, most of them overlooked the deployment position or preset candidate position (Liao et al., 2014; Ejaz et al., 2015).

In this paper, we attempt to deploy fixed chargers without any candidate positions in 3D scenario, namely to determine their number, transmitting power and deployment location, where the information of sensors including position and energy consumption is known. Generally speaking, the greater the total transmitting power of chargers, the higher the received power of nodes. However, we hope that the sensors receive larger power with the minimum total transmitting power of the charger, that is, a higher charging benefit is obtained at a lower cost. Therefore, the received power and the total transmitting power should be optimized simultaneously. To address this issue, the Fixed Charger Deployment problem (FCD) is formulated as a multi-objective optimization problem.

FCD is similar with the coverage problem in traditional wireless sensor networks, while the existing solutions cannot be used directly in our research for the following two reasons. Firstly, the direction of signal transmission is different. In our problem, the sensor node receives the RF signal from the charger, while the traditional coverage problem deploys the sensor node to sense the target states. Secondly, the wireless charging models are different from the coverage models in the traditional wireless sensor network which can be classified as physical coverage and probabilistic coverage. Physical model refers to specific deployment topology, and the target points in the region can be monitored by at least one sensor node. Probabilistic model utilizes probabilistic statistical methods to predict the possibility of target points being monitored. These two models are distinct from the wireless charging model. Moreover, due to the non-linearity of FCD, traditional optimization methods are difficult to solve it. Therefore, a multi-objective optimization genetic algorithm based on NSGA2 is proposed.

An original approach is presented for WRSN system modelling for control purpose. On one hand, this specification can quantitatively represent the energy and control flow in the charging process. On the other hand, the position relationship between the chargers and the sensors should be visually demonstrated. With both mathematical and graphical presentation features, Petri nets are competent. While both classical Petri net and other Petri nets for traditional wireless sensor network can't describe such complex hybrid system. Therefore, it is necessary to extend the Petri net to characterize these properties comprehensively. For example, cyber Petri nets are used to control charging behaviour, and coloured Petri nets are used to classify different "resources" in the system. Based on the above analysis, Generalized Synchronizing Coloured Cyber Petri Nets (GSCCPN) is proposed to formalize the charging deployment in WRSN.

The contributions are summarized as follows. To the best of our knowledge, it is the first work that Petri net is applied for WRSN, and the Generalized Synchronizing Coloured Cyber Petri Nets is presented, which can express energy flow, control flow, and position flow. Secondly, FCD is formulated as a multi-objective optimization problem without candidate positions for the first time. It has been proved to be NP-hard (NP-Hardness, non-deterministic polynomial-time hardness). A multi-objective optimization genetic algorithm is proposed to obtain the sub-optimal solution. Finally, the proposed algorithm is evaluated by large-scale simulation, and the impact of factors such as the number of chargers, node energy consumption, and number of nodes on deployment are studied.

The remainder of the paper is organized as follows. Section 2 reviews some related works on wireless charger deployment and Petri nets. Section 3 constructs the charging model based on Petri nets. Section 4 proposes the charger deployment strategy. Section 5 evaluates the efficiency of the proposed algorithm. Section 6 concludes the paper.

2. RELATED WORK

2.1 Charging Deployment in WRSN

In recent years, some scholars have studied the deployment of wireless chargers. He et al. divided the charger deployment into static and dynamic ones, which involved point provisioning and path provisioning respectively. They were deployed in the vertex of equilateral triangles, and the number of chargers was reduced as much as possible by expanding the triangular area. The proposed point provisioning has been proved to be able to achieve sub-optimal performance, while the path provisioning is actually close to the optimal performance (He et al., 2013). On the background of 3D beam directed antenna, Liao et al. proposed two greedy algorithms, namely, greedy cone selection algorithm (NB-GCS) based on nodes and greedy cone selection algorithm (PB-GCS) based on node pair, assuming that chargers are deployed in fixed height grids. The latter is superior to the former in the number of nodes, while the complexity of the former is lower (Liao et al., 2014). To optimize the deployment and quantity of chargers, Ejaz et al. used the trade-off coefficient to balance charging optimization and energy fairness (Ejaz et al., 2015). Lin et al. developed the deployment strategy of the charger when the energy consumption of the nodes was not uniform (Lin et al., 2016). Lai et al. sought the optimization goal of minimum charger position and shortest charging time. A two-step solution was proposed to minimize the number of charger positions and then allocate residence time according to charging requirements. Compared with the minimum group partition scheme, the number of charging positions and the total charging time can be saved by 60% (Lai and Hsiang, 2019). Nicolae et al. studied the utility of directional antennas and synchronization mechanism for prolonging the life of the sensor nodes from a ground deployed WSN. It was proved through simulation that the node's life is desired to reach several years (Nicolae et al., 2016). Yang et al. proposed a firefly algorithm based on adaptive attraction factor and dynamic position updating mechanism to deploy chargers. Simulation results showed that the IFA algorithm is superior to several reference algorithms for comparison in terms of accuracy and convergence speed (Yang et al., 2018).

In addition to charging efficiency, electromagnetic radiation safety is also considered. In order to ensure that the electromagnetic radiation intensity at any point in the charging area is less than a given threshold R_t, Dai et al. put forward a safe charging problem for charger scheduling(SCP), which maximizes the charging effectiveness within the safe threshold range of electromagnetic radiation. The gap between the maximum electromagnetic radiation point algorithm and the optimal algorithm is only 6.7, which is 34.6% better than the greedy algorithm (Dai et al., 2017). To adjust the transmitting power continuously, the optimization problem was transformed into the traditional linear programming, and the redundant constraints were removed, and a series of distributed algorithms were designed. Simulation results showed that the average performance of the overall charging utility is 41.1% better than the existing algorithms (Dai et al., 2018). Then, Li et al. proposed a region segmentation algorithm to reduce the transmission power to a safe threshold, so that the lowest energy utility nodes were maximized (Li et al., 2019). Sheikhi et al. put forward a solution for the combination of mobile charger and fixed charger. The fixed charging station uses grid elements to form a virtual area, and the charging stations coordinate with each other to guide the mobile chargers in the area (Sheikhi et al., 2019).

However, the above researches only focused on the number of chargers or scheduling strategies, and locations of deployment were uninvolved or preset via candidate locations.

2.2 The application of Petri Nets

Due to the integration of mathematics and graphic representation, Petri nets have unique advantages in network modelling, especially in production scheduling, transportation network and so on, providing a unified environment for modeling, behavioral attributes, and performance analysis. Li et al. built the production scheduling of flexible manufacturing system (FMS) by using time-delay petri nets, and obtained the optimal scheduling strategy by means of heuristic algorithm (Li et al., 2015). Kadri et al. proposed a variable arc weight Petri net to solve the scheduling of shared bicycles, and used genetic algorithm to ensure that bicycles are available for pick up and vacant berths available for bicycle drop off at every station (Kadri et al., 2015). Gonsalves et al. dealt with the performance modeling and the optimization of concurrent service systems, and demonstrated the effectiveness of the novel Client Server Petri net model editor–simulator–optimizer with the practical example of an automobile purchase concurrent service system (Gonsalves and Itoh, 2011). Wan et al. proposed a new approach for the modeling and VHDL implementation of digital systems based on an extended class of Petri nets and defined the generalized synchronous self-modifying net (GSSN) to describe digital systems. (Wan et al., 2017). G. Y. Zhang et al. implemented a multi-component collaborative design methodology for a liquid rocket engine and took Petri nets for performance driven design process based on extended Petri nets which can effectively couple existing knowledge resources, solve any conflict arising from different knowledge, and achieve an optimal strategy (G. Y. Zhang et al., 2017) .

Although Petri nets are widely used in many fields, they only play a relatively minor role in the modeling and analysis of wireless sensor networks, and mainly used for the analysis and prediction of sensor nodes' energy. Mateo et al. used Prioritized-Timed Colored Petri Nets (PTCPNs) to model routing behavior in WSN, and proposed a new routing algorithm to reduce node energy consumption and improve data routing (Mateo et al., 2014). Zeng et al. constructed a Stochastic Petri Net to analyze the performance of WSNs (Zeng and Hong, 2009). Sousa, J. R. B et al. present Differential Hybrid Petri Nets to model, to simulate and to analyze the energy consumption of a sensor node (Sousa et al., 2005). Yu, Z. H et al. used fuzzy Petri nets to select cluster heads and compute the degree of reliability in the route sprouting tree from cluster heads to the base station (Yu et al., 2011). Zairi, S et al. proposed a modeling approach considering the global behavior of a sensor network and allowing the estimation of network's energy consumption based on Colored Petri Nets (Zairi et al., 2015).

The Petri net model established in this paper not only considers the energy information of the sensor nodes, but also contains the node's position and control relationships. The gap of Petri nets in WRSN is to be filled in this paper.

3. PROBLEM FOMULATION

3.1 Charger Deployment Modelling

Fixed chargers are deployed in complex terrain conditions, hence assuming that there is a set of m static chargers $C=\{c_1,c_2,\cdots,c_m\}$ and n sensor nodes $S=\{s_1,s_2,\cdots,s_n\}$ in a three-dimensional space. The nodes can receive power from the chargers and thus maintain normal operation. In this paper, Friis' free space equation is used as the wireless charging model (He et al., 2013), namely,

$$P(d_{ij})=\frac{G_S G_r \eta}{L_p}\left(\frac{\lambda}{4\pi(d_{ij}+\beta)}\right)^2 p_i \tag{1}$$

where d_{ij} represents the Euclidean distance between charger i and node j, G_S is the source antenna gain, G_r is the receive antenna gain, λ is the wavelength, L_p is polarization loss, and η can be referred to as rectifier efficiency, β is a parameter to adjust the Friis' free space equation. Since all the above parameters are constants, equation (1) can be simplified to (2),

$$P(d_{ij})=\frac{\tau}{(d_{ij}+\beta)^2}\cdot p_i \tag{2}$$

where $\tau=\frac{G_S G_r \eta}{L_p}\left(\frac{\lambda}{4\pi}\right)^2$, the coordinates of charger and sensor node are respectively $(x_i,y_i,z_i),(x_j,y_j,z_j)$, then $d_{ij}^2=(x_j-x_i)^2+(y_j-y_i)^2+(z_j-z_i)^2$, p_i represents the transmitting power of i^{th} charger.

It can be seen that the greater the transmitting power and the smaller the distance from the charger, the more power a sensor node receives and vice versa. Since the power received varies with the location of the charger, FCD is fundamentally different from the traditional wireless sensor network coverage. It is expected that the charger will emit as little power as possible, while the network utility will be as effective as possible. Network utility can be defined as,

$$u(s_j)=\sum_{i=1}^{m}P(d_{ij}) \tag{3}$$

With the aforementioned models, FCD can thus be described and mathematically formulated as follows:

$$\min\ \sum_{i=1}^{m}p_i,\max\ \sum_{j=1}^{n}u(s_j)$$
$$s.t.\ \forall u\in\mathbb{R}^2,\quad l_j\le u(s_j) \tag{4}$$

The constraint condition indicates that the network utility cannot be less than the power consumption of the node, and l_j represents the consumption power of j^{th} node.

It is very challenging from the above formulation. Since the location of deployable chargers is infinite, in other words, there may be an infinite number of chargers, which makes it extremely difficult to analyze. Moreover, even if the number of chargers can be reduced, the power matching is still a knapsack problem, and the knapsack problem is NP hard.

3.2 Petri Nets Modelling

In its basic form, a Petri net is a directed graph with places and transitions. Places and Transitions are connected by directed arcs. A transition can only be fired, if each of the input places of this transition contains at least one token. Due to the lack of describing the control behavior and resource types, the classic Petri net should be extended.

Therefore, Generalized Synchronizing Colored Cyber Petri Nets (GSCCPN) is proposed for modelling, and the definition will be given below.

Definition 1 The condition that six-tuple $\sum(S,T;F,K,W,M_0)$ containing k colors constitutes GSCCPN is

① $\mathrm{N}=(S,T;F)$, named as a basic Petri net.

② K is the capacity function of N.

③ W is weight function of N, representing a K-dimensional nonnegative vector assigned to each directed arc.

④ M_0 is the initial marking.

Definition 2 The condition of transition firing is

M is the marking of N, $t\in T$

Supposing that the marking $M(s)$ contains 4 colors, and $M(s)=[x,y,z,p]=[M(s)_1,M(s)_2,M(s)_3,M(s)_4]$

① $\forall s\in {}^{\cdot}t:M(s)_4\ge W(s,t)_4\wedge\forall s\in t^{\cdot}:\ M(s)_4+W(t,s)_4\le K(s)_4$

If transition t is fired, it can be recorder as M [t > .

② If transition t is fired on M, M can be changed to be M', and M' is given as follows.

$$M'(s) = \begin{cases} [M(s)_1, M(s)_2, M(s)_3, M(s) - W(s,t)] & s \in {}^{\bullet}t - t^{\bullet} \\ [M(s)_1, M(s)_2, M(s)_3, M(s) + W(t,s)] & s \in t^{\bullet} - {}^{\bullet}t \\ [M(s)_1, M(s)_2, M(s)_3, M(s) - W(s,t) + W(t,s)] & s \in {}^{\bullet}t \cap t^{\bullet} \\ M(s) & s \notin ({}^{\bullet}t \cap t^{\bullet}) \end{cases} \quad (5)$$

The relationship between M and M' is denoted by M [t > M'.

The state equation of GSCPN can be written as

$$M' = M_0 + \rightarrow C \cdot U \quad (6)$$

where the matrix operator $+\rightarrow$ represents the substitution plus, C is the incidence matrix, and U is the matrix representation of the sequence of concurrent steps $U_1 U_2 \cdots U_k$.

Hence, the state equation of GSCCPN can be written as

$$M(t_n) = M_0 + C \cdot \left[\int_{\tau_0}^{\tau_n} ()\right] d\tau \quad (7)$$

Definition 3 A read arc is a directed arc with an arrow in the middle from the place to the transition. The weight of read arc is 0. After the transition fired from the read arc, the marking of the input place is unchanged.

Definition 4 A write arc is a directed arc with an arrow in the middle from the transition to the place. The write arc is a special weighted control arc. After the transition fired, the output place is updated to the value of the weight.

Fig. 1 shows a simple GSCCPN. The initial marking is $M_0 = ([x_1, y_1, z_1, p_1],\ [x_2, y_2, z_2, 0])$. The new marking after firing is $M_1 = ([x_1, y_1, z_1, p_1],\ [x_2, y_2, z_2, W(T_{12}, S_2)])$ by transition firing condition. The arc weight $W(T_{12}, S_2)$ is variable and the marking of place S_1 is unchanged.

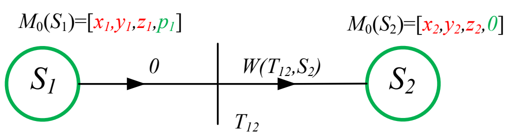

Fig. 1. Generalized Synchronizing Colored Cyber Petri Nets, GSCCPN.

The GSCCPN model of FCD is shown in Fig. 2, and the important symbols are shown in Table 1.

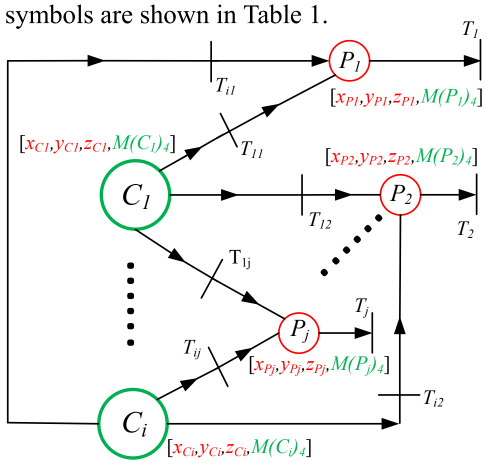

Fig. 2. GSCCPN model of FCD.

Here, The place C_i and P_j represents charger and sensor node respectively, where the red markings indicate the 3D coordinates, while the green marking indicates the transmitting power or the received power. From the above definition, $W(T_{ij}, P_j)$ is the harvesting power of j^{th} sensor node from the i^{th} charger, and $W(T_{ij}, P_j) = \frac{\tau}{(d_{ij}+\beta)^2} \cdot p_i$, $l_j = W(P_j, T_j)$. It is can be known that with the change of place C_i (represent the position and transmitting power of i^{th} charger), the arc weight $W(T_{ij}, P_j)$ will change accordingly.

Table 1. List notations.

Notation	Definition
C_I	i^{th} Charger
P_j	j^{th} Sensor node
T_{ij}	The j^{th} Sensor node is charged by i^{th} Charger
T_j	The j^{th} Sensor node is consuming power

The GSCCPN dynamic equation of FCD can be expressed as

$$M(P_j)_4 = \left[\sum_{i=1}^{m} W(T_{ij}, P_j) - W(P_j, T_j)\right] \cdot \left[\int_{\tau_0}^{\tau_n} ()\right] d\tau \quad (8)$$

It can be seen that the following conditions must be satisfied in order to ensure sufficient energy of sensor nodes,

$\sum_{i=1}^{m} W(T_{ij}, P_j) - W(P_j, T_j) \geq 0$. Hence, the GSCCPN of FCD is mathematically formulated as follows:

$$\min \sum_{i=1}^{m} M(C_i)_4, \max \sum_{j=1}^{n} W(T_{ij}, P_j)$$
$$s.t.\quad \sum_{i=1}^{m} W(T_{ij}, P_j) \geq W(P_j, T_j) \quad (9)$$

In summary, the position, energy, and charging control relationship in WRSN can be fully illustrated and explained by GSCCPN. Compared with the Hybrid Petri net, GSCCPN introduces location information, and assigns different colors to the marking, with the ability to describe different "resources", so as to model FCD for WRSN.

4. CHARGER DEPLOYMENT OPTIMIZATION

The two optimization objectives of FCD are conflict with each other, that is, the optimal solution cannot be achieved at the same time, hence it is necessary to make a trade-off between the two objectives. However, the problem is NP hard, and the traditional optimization method is difficult to solve. Therefore, A Charger Deployment Multi-Objective Optimization Genetic Algorithm (CDMOGA) based on NSGA2 is proposed. Assuming that all sensor nodes in the network can receive the power emitted by the chargers.

4.1 NSGA2 Algorithm

NSGA2 is one of the most popular algorithms. By means of fast non-dominate sorting algorithm, crowded competition selection method and elite strategy, the Pareto optimal solution can be searched efficiently. This method guarantees the diversity of population and prevents individual loss. The principle of the standard NSGA2 algorithm is as follows.

The initial population D_t is randomly generated and sorted according to different non-dominate hierarchies. A fitness value equal to the non-dominant level is assigned to each solution. Binary tournament selection, mutation and recombination operators are used to generate offspring population. Then the following steps is repeated until the number of iterations reach the maximum.

Step1. Combine the parents and offspring populations, and create $P_t = D_t \cup E_t$. According to algorithm 1, perform fast non-dominant sorting in P_t and identify different frontiers Fr_i.

Step2. Set a new population $D_{t+1} = \emptyset$, and let $counter\ i = 1$. $While\ |D_{t+1}| + |Fr_i| < N, do\ D_{t+1} = D_{t+1} \cup Fr_i\ and\ i = i + 1$.

Step3. Choose (N-$|D_{t+1}|$)most general solution from binary crowding tournament selection operator, and insert them into D_{t+1}.

Step4. Create offspring E_{t+1} from D_{t+1} by binary crowding tournament selection, crossover and mutation operators, and let $t = t + 1$.

Fast non-dominate sorting algorithm
Input: population P
Output: The non-dominated fronts $(Fr_1, Fr_2, \cdots)$

For each $p \in P$
  For each $q \in P$
    If $(p < q)$ then
      $S_p = S_p \cup \{q\}$
    else if $(q < p)$ then
      $n_p = n_p + 1$
    If $n_p = 0$ then
      $F_1 = F_1 \cup \{p\}$
$i = 1$
while $F_i <> \emptyset$
  $H = \emptyset$
  For each $p \in Fr_i$
    For each $q \in S_p$
      $n_q = n_q - 1$
      If $n_q = 0$ then $H = H \cup \{q\}$
$i = i + 1$
$Fr_i = H$

Algorithm1: The pseudocode of fast non-dominate sorting algorithm

The non-dominant sorting process and the steps to fill the population D_{t+1} can be performed together. The crowd ordering of solutions in frontier Fr_i is performed by crowding distance, while Fr_i is the last frontier which cannot be fully accommodated.

The crowding comparing operator compares two solutions and returns the victor. The choice is based on the following two points: non-dominate ranking r_i and the local crowding distance within the population. The crowding distance of solution i is the measurement of the search space around i, which is not occupied by any other solution in the population. Based on r_i and d_i, the binary crowding tournament selection operator works as follows.

Solution i beats solution j in the race if the following conditions are true.

(1) If $r_i < r_j$ (This condition ensures that the selected solution lies in a more non-dominant position).

(2) If $r_i < r_j$ and $d_i < d_j$ (When both solutions are on the same front and the above conditions cannot be applied, the method is applied; in this case, the solution in a less crowded area wins).

4.2 Dynamic crowding distance Algorithm

The horizontal diversity of the Pareto frontier is very important in multi-objective optimization, which is achieved by eliminating the redundant individuals in the dominance concentration. To remove redundant individuals, NSGA2 uses crowding distance measurement. The removed individuals with lower crowding distance values have a higher priority. The crowding distance value is calculated by the following formula,

$$CD_i = \frac{1}{N_{obj}} \sum_{z=1}^{N_{obj}} |F_{i+1}^z - F_{i-1}^z| \quad (10)$$

Here, N_{obj} is the number of objectives, F_{i+1}^z is z^{th} objective of *i+1* individual, F_{i-1}^z is the z^{th} target of the $(i-1)^{th}$ individual after sorting the population according to the crowding distance value. The main defect of crowded distance is lack of uniform diversity in obtaining non-dominated solutions. A dynamic crowding distance algorithm was proposed (Luo et al., 2008). The dynamic crowding distance of individuals is:

$$DCD_i = \frac{CD_i}{\log(1/Var_i)} \quad (11)$$

CD_i can be obtained by (10), and Var_i can be obtained by (12),

$$Var_i = \frac{1}{N_{obj}} \sum_{z=1}^{N_{obj}} (|F_{i+1}^z - F_{i-1}^z| - CD_i)^2 \quad (12)$$

Var_i is the variance of the crowded distance between the *ith* neighbouring individuals.

4.3 Genetic representation of the algorithm

In the traditional genetic algorithm, chromosomes are represented by binary strings. In order to calculate the value of the objective function, the binary strings (genotypes) need to be converted to the real number space (phenotypes), which will inevitably increase the calculation cost. Therefore, a more effective real number representation method is adopted in this paper, which is a direct coding mechanism, and the genotype and phenotype are exactly the same. As shown in Fig. 2, each place contains 4 markings. Hence, every charger gene is represented by a four-digit vector, the first of which represents the transmitting power of the charger, and the last three represent the three coordinates of the charger, as shown in Fig. 3.

C_1	C_2		C_i
$M(C_1)_4$ & x_{C1}, y_{C1}, z_{C1}	$M(C_2)_4$ & x_{C2}, y_{C2}, z_{C2}	……	$M(C_i)_4$ & x_{Ci}, y_{Ci}, z_{Ci}
Gene1	Gene 2		Gene N

Fig. 3. Genetic representation of the algorithm.

4.4 Charger Deployment Multi-Objective Genetic Algorithm

In the first, an initial population of size M is generated. G places of the chargers are uniformly distributed randomly, the marking of the sensor place $M(P_j)_4$ is computed, and the objective function is obtained under the constraint condition. Then offspring are created from existing populations through crowded race selection, crossover, and mutation operators.

Charger Deployment Multi-Objective Genetic Algorithm (CDMOGA)

Input： markings of sensor place

Output： Non-dominate solution

Step 1. Choose population of size M, crossover probability (P_C)and mutation probability (P_M), maximum iterations (gen_{max}), Set the iteration count from t=0;
Step 2. Generate initial population D_t according to the rules below
For $i = 1, \cdots, M$ do
Step 2.1. Generate G places of the chargers randomly
Step 2.2. Assign transmitting power marking and position marking for each place of charger;
Step 3. Evaluate each solution of the initial population according to the objective function and constraints;
Step 4. Create offspring population E_t by crowding tournament selecting, crossover and mutation in D_t;
Step 5. Let $P_t = D_t \cup E_t$;
Step 6. Perform fast non-dominate sorting for P_t, and generate non-dominate frontiers $Fr_1, Fr_2, \cdots$;
Step 7. Set $D_t + 1 = \emptyset$; $i = 1$;
While $|D_{t+1}| + |Fr_i| < M$ do
$(D_{t+1} = D_{t+1} \cup Fr_i, i = i + 1)$;
If $|D_{t+1}| < M$ then
Calculate DCD in Fr_i, and arrange them in descending order, Add the first solution $M - |D_{t+1}|$ to D_{t+1} from Fr_i;
If $t < gen_{max}$ then set $t = t + 1$, and return to Step 3.

Algorithm2: The pseudocode of CDMOGA

A two-point crossover operator is designed, and the crossover point can be randomly selected between variables. The crossover rule is:

(1) Select the first m vectors from the first parent chromosome;

(2) choose the vector between m+1 and n from the second parent;

(3) choose the vector after the *nth* from the first parent chromosome;

These operators then combine genes to form a new progeny. For example, p1 and p2 are the parent chromosomes,

p1 = [a b c d e f g h], p2 = [1 2 3 4 5 6 7 8],

If the intersection is between the third and sixth positions, then the offspring chromosome is:

child = [a b c 4 5 6 g h],

Some genes will be randomly selected for mutation after crossover, which can introduce features not belonging to the original population and prevent the algorithm from too fast convergence. Mutation operators usually select a pair of genes on the chromosome and flip their positions. A sliding mutation operator is developed in this paper, as shown in Fig. 4. Let x_{min} and x_{max} represent the minimum and maximum value of genes, and x is the current gene value. Slide direction is selected randomly, right or left, and the slide momentum is generated arbitrarily within the allowed range. However, the gene mutated by sliding cannot cross the boundary. Thus, the boundary conditions of the decision variables remain unchanged. In other words, lethal genes are always avoided.

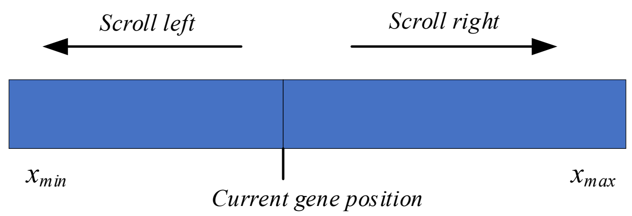

Fig. 4. Mutation Operator.

The offspring population is combined with the parent population. Then, a fast non-dominate sorting algorithm is applied to the combined population to identify different frontiers Fr_i $i = 1,2, \cdots$. And the new population contains the solutions of different non-dominant fronts.

A new population of size M may not be able to accommodate all the frontiers of a combined population of size 2M. Therefore, if all solutions of the existing frontier cannot be accommodated by the new population, the dynamic crowding distance in the new population will be calculated. Then the solution is sorted in descending order according to the dynamic crowding distance, and the solution required by the new population will be selected from the first one at the frontier. The above process continues until the maximum iterations is reached. Algorithm 2 shows the pseudocode of CDMOGA.

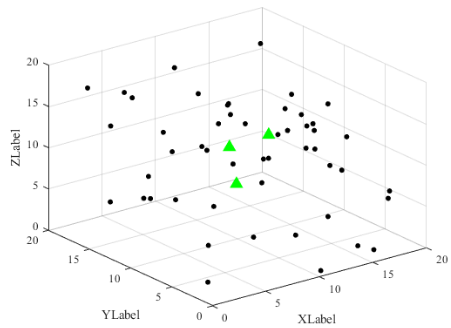

(a)

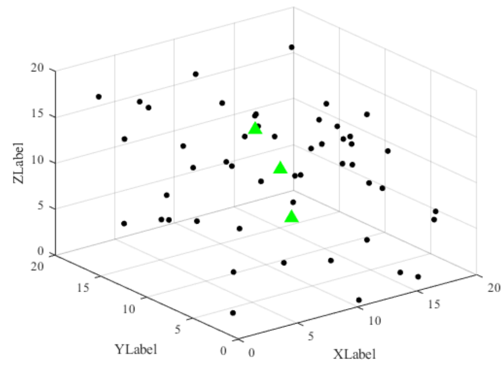

(b)

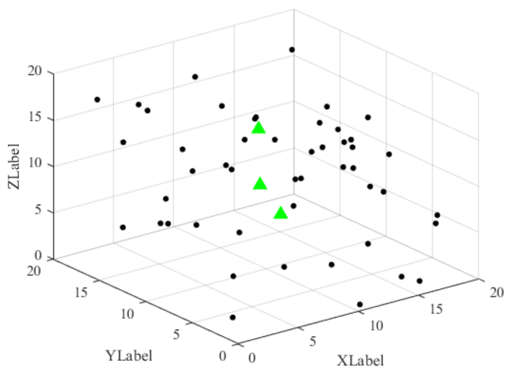

(c)

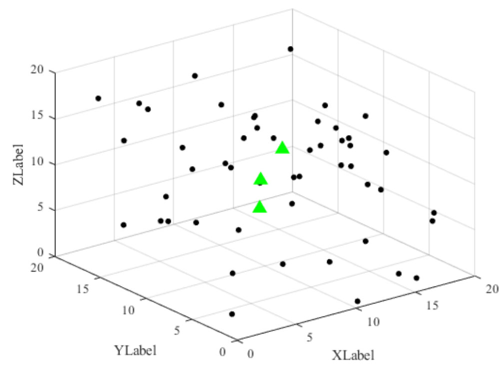

(d)

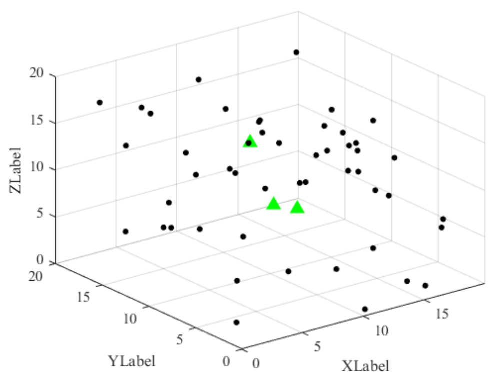

(e)

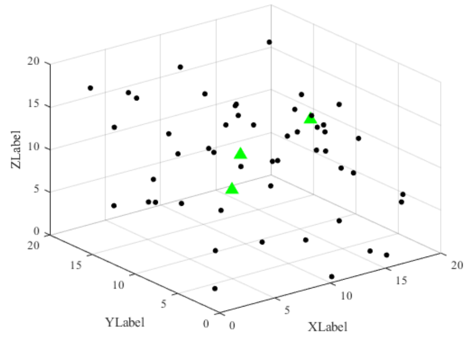

(f)

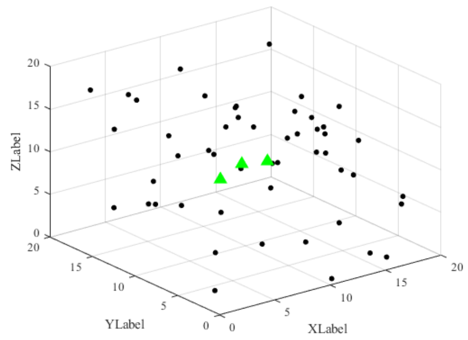

(g)

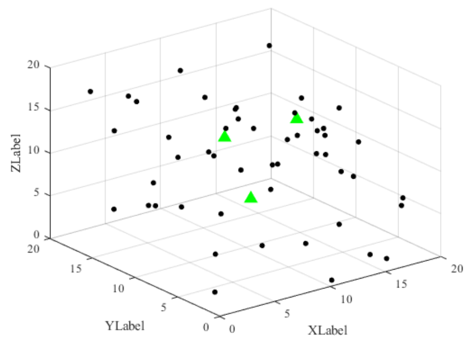

(h)

Fig. 5. 3 chargers deployment scheme of 50 nodes. (a)~(h) corresponds to scheme 1-8, respectively.

5. SIMULATION AND ANALYSIS

In this section, large scale simulation is conducted by MATLAB 9.0 and the algorithm performance will be evaluated.

5.1 Simulation settings

The experiment is carried out in a solid space with a side length of 20 meters. It is assumed that all sensor nodes in the space can receive the energy emitted by the charger, and the energy reception is additive for different chargers. Moreover, each point on the simulation curve represents the average of 50 simulation results. $G_S = 8\,dBi$, $G_r = 2\,dBi$, $\lambda = 0.33$, $\eta = 0.125$, $L_p = 0.5$, $\beta = 0.125$. Other parameters are shown in Table 2.

Table 2. Simulation parameters.

Parameters	Description
WRSN cuboid	$20\text{M}(L) \times 20\text{M}(W) \times 20\text{M}(H)$
Number of sensor nodes	10，20，30，40，50
Number of Chargers	1,2,3,4,5,6,7,8
Node Distribution	Uniform Distribution
Power consumption	50μw

5.2 Results

Fig. 5 shows eight schemes for the deployment of 3 chargers under the random distribution of 50 sensor nodes, where the sensor node is represented by black solid dots and the green triangle represents the charger. And the chargers is basically deployed in the same area.

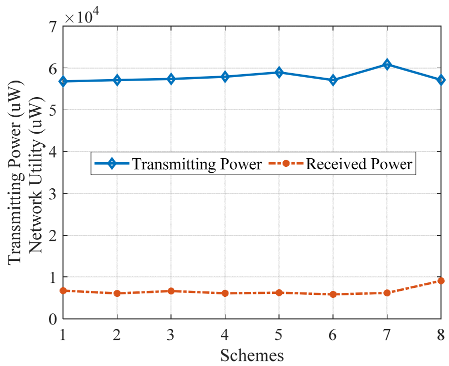

Fig. 6. Transmitting power and Received power of 8 schemes.

As can be seen from Fig. 6, the transmission power is not the same, While the total transmission power of the eight schemes is basically the same. This shows that although this algorithm can only obtain an optimal solution set, rather than a single optimal solution, the difference between different solutions is very small, which can effectively solve the charger deployment problem.

Furthermore, the results also show that the genetic algorithm is able to schedule the GSCCPN, demonstrating the feasibility of this specification.

5.3 Performance comparison

CDMOGA is compared with MOEA/D (Q.

(F. Zhang and Li, 2007), SPEA2 (Zitzler and Thiele, 1999), and the following metrics for evaluation is considered:

(1) influence on receiving power and transmitting power with different nodes;
(2) influence on transmitting power with different power consumption;
(3) influence on transmitting power with heterogeneous nodes;
(4) influence on receiving power and transmitting power with different chargers.

Experiment 1. When the number of sensor nodes increases from 10 to 50, the receiving power and the transmission power are shown in Fig. 7 and Fig. 8, respectively. As can be seen in Fig. 7, the total received power is increased with the number of nodes, since in the case of a constant number of chargers and transmission power, the sensor nodes become more, i.e., the charged device is increased, so that the power received by the network is also increased. Fig. 8 shows the trend of transmission power changing with the number of sensor nodes. In general, the more sensors there are, the greater the transmission power is required. The reason is that the probability of the sensor nodes distributed to the region's edge is positively correlated with their own number. In addition, the transmission power of CDMOGA is 6% and 7.8%lower than that of MOEA/D and SPEA2, respectively, and the receiving power is 17.6% and 25.2% higher than that of latter. This is due to the fact that CDMOGA is more inclined to the elite strategy in the deployment strategy, so that the charger has lower transmission power and sensor nodes can receive higher power.

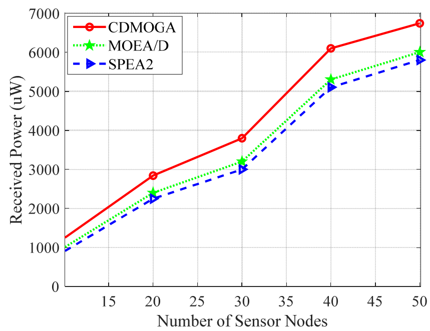

Fig. 7. Received power with the different sensor nodes.

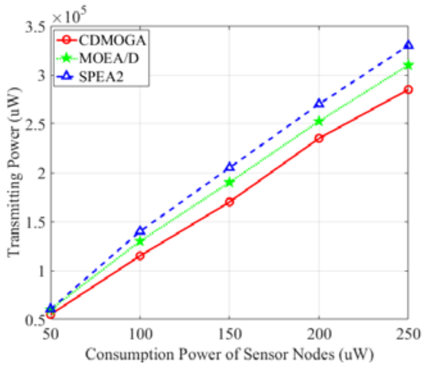

Fig. 8. Transmitting power with the different sensor nodes.

Experiment 2. The experiment simulates the trend of transmission power when the power consumption of sensor nodes increases from 50 to 250. As shown in Fig. 9, the transmission power of the CDMOGA is increased from 57 mW to 285 mW, and the transmission power generated by MOEA/D and SPEA2 is increased from 62 mW, 63 mW to 310 mW, 330 mW, respectively, which reflects that the transmission power tends to increase with node power consumption, while the ther two algorithms are 9.3% and 14.3% higher than CDMOGA, respectively. Therefore, the performance improvement of CDMOGA is more obvious as the node power consumption increases.

Experiment 3. In this experiment, the distribution position and number of the sensor nodes are unchanged, and the power consumption of 10 nodes is increased to 100μW, as shown by the black square in Fig. 10, and the power consumption of the remaining nodes is maintained at 50μW. The green triangle and the red pentagram represent the charger deployment position before and after the power consumption change, respectively. Since seven nodes with larger power consumption are on the right side of the region, two chargers are obviously moved to the right. At the same time, there are still 3 nodes with higher power consumption on the left side of the region, hence one charger remains in the original deployment area to ensure that the remaining left-hand nodes are not affected. Moreover, after the node power consumption changes, the transmitting power of the charger increases from 57mW to 100mW, almost doubled. It can be seen that even if the power consumption of a small number of nodes increases, the transmission power will increase significantly due to the superposition effect of position.

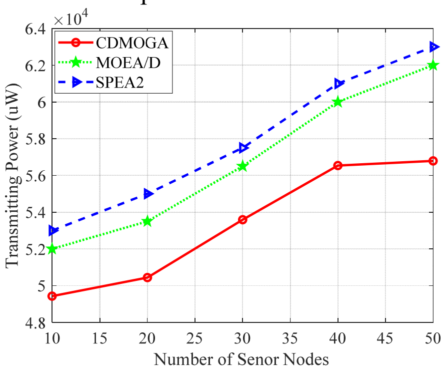

Fig. 9. Transmitting power with the different node power consumption.

Experiment 4. This experiment evaluates the influence of the number of chargers on the transmission power. As shown in Fig. 11, the number of chargers increases from 1 to 8. When a single charger is deployed, its transmission power increases slightly because it is difficult to take into account all sensor nodes, but there is no significant change in the transmission power and reception power in the rest cases. The experimental results show that there is no obvious relationship between the number of chargers and the total transmission power. As long as the threshold of transmission power of a single charger is not exceeded, the number of chargers can be reduced as much as possible in order to reduce the deployment difficulty and maintenance cost.

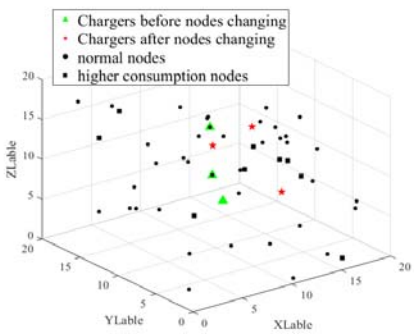

Fig. 10. Charger deployment with heterogeneous nodes.

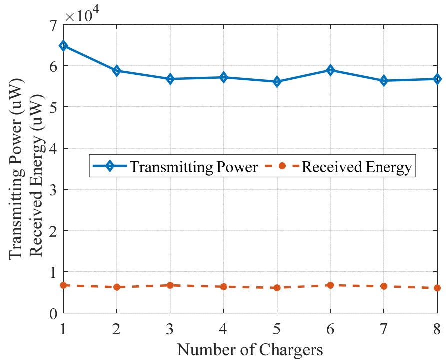

Fig. 11. Charger deployment with heterogeneous nodes.

6. CONCLUSIONS

The paper innovatively proposes a generalized synchronizing colored cyber Petri net (GSCCPN) to model the fixed charger deployment in WRSN. And this issue is studied without candidate positions in 3D scenario for the first time. To make a tradeoff between two conflict objectives, the algorithm CDMOGA based on NSGA2 is proposed. The results show that the genetic algorithm is able to schedule the GSCCPN. And numerical simulation verifies the rationality and feasibility of the algorithm. The future work will be focused on extending the field to hybrid charging and crowd charging in 5G scenario.

ACKNOWLEDGMENTS

This work was supported by National Natural Science Foundation of China under Grant [NO. 61070058].

REFERENCES

Alqahtani, M., Gumaei, A., Mathkour, H., and Ben Ismail, M. M. (2019). A Genetic-Based Extreme Gradient Boosting Model for Detecting Intrusions in *Wireless Sensor Networks. Sensors,* 19(20), 20. doi:10.3390/s19204383

Dai, H. P., Liu, Y. H., Chen, G. H., Wu, X. B., He, T., Liu, A. X., & Ma, H. Z. (2017). Safe Charging for Wireless Power Transfer. *Ieee-Acm Transactions on Networking*, 25(6), 3531-3544.

Dai, H. P., Liu, Y. H., Chen, G. H., Wu, X. B., He, T., Liu, A. X., and Zhao, Y. (2018). SCAPE: Safe Charging With Adjustable Power. *Ieee-Acm Transactions on Networking*, 26(1), 520-533.

Dominguez-Morales, J. P., Rios-Navarro, A., Dominguez-Morales, M., Tapiador-Morales, R., Gutierrez-Galan, D., Cascado-Caballero, D., Linares-Barranco, A. (2016). Wireless Sensor Network for Wildlife Tracking and Behavior Classification of Animals in Donana. *IEEE Communications Letters*, 20(12), 2534-2537. doi:10.1109/lcomm.2016.2612652

Ejaz, W., Kandeepan, S., and Anpalagan, A. (2015, Aug. 30 2015-Sept. 2 2015). Optimal placement and number of energy transmitters in wireless sensor networks for RF energy transfer. Paper presented at the Personal, Indoor, and Mobile Radio Communications (PIMRC), *2015 IEEE 26th Annual International Symposium on*.

Gonsalves, T., and Itoh, K. (2011). GA optimization of Petri net-modeled concurrent service systems. *Applied Soft Computing, 11*(5), 3929-3937.

He, S., Chen, J., Jiang, F., Yau, D. K. Y., Xing, G., and Sun, Y. (2013). Energy Provisioning in Wireless Rechargeable Sensor Networks. *Ieee Transactions on Mobile Computing*, 12(10), 1931-1942.

Kadri, A. A., Labadi, K., & Kacem, I. (2015). An integrated Petri net and GA-based approach for performance optimisation of bicycle sharing systems. *European Journal of Industrial Engineering,* 9(5), 638-663. doi:10.1504/ejie.2015.071777

Lai, W. Y., and Hsiang, T. R. (2019). Wireless Charging Deployment in Sensor Networks. *Sensors*, 19(1), 19.

Li, L. L., Dai, H. P., Chen, G. H., Zheng, J. Q., Dou, W. C., and Wu, X. B. (2019). Radiation Constrained Fair Charging for Wireless Power Transfer. *Acm Transactions on Sensor Networks*, 15(2), 33.

Li, C., Wu, W. M., Feng, Y. P., and Rong, G. (2015). Scheduling FMS problems with heuristic search function and transition-timed Petri nets. *Journal of Intelligent Manufacturing*, 26(5), 933-944.

Liao, J.-H., Jiang, J.-R., and Ieee. (2014). Wireless Charger Deployment Optimization for Wireless Rechargeable Sensor Networks. *2014 7th International Conference on Ubi-Media Computing and Workshops (Umedia)*, 160-164.

Lin, T. L., Li, S. L., and Chang, H. Y. (2016). A Power Balance Aware Wireless Charger Deployment Method for Complete Coverage in Wireless Rechargeable Sensor Networks. *Energies, 9*(9), 13.

Lloret, J., Garcia, M., Bri, D., and Sendra, S. (2009). A Wireless Sensor Network Deployment for Rural and Forest Fire Detection and Verification. Sensors, 9(11), 8722-8747. doi:10.3390/s91108722

Luo, B., Zheng, J., Xie, R., and Wu, J. (2008). Dynamic Crowding Distance-A New Diversity Maintenance Strategy for MOEAs.

Mateo, J. A., Ruiz, M. D., Macia, H., and Pardo, J. J. (2014). Formal Study of Routing Protocols for Wireless Sensor Networks. *Journal of Universal Computer Science*, 20(9), 1373-1401.

Nicolae, M., et al. (2016). "Scheduling Mechanism for Energy-Efficient Communication in Hybrid Wireless Sensor Networks." *Control Engineering and Applied Informatics,* 18(2): 95-102.

Sheikhi, M., Kashi, S. S., and Samaee, Z. (2019). Energy provisioning in wireless rechargeable sensor networks with limited knowledge. *Wireless Networks*, 25(6), 3531-3544.

Sousa, J. R. B., Lima, A. M. N., and Perkusich, A. (2005, 6-10 Nov. 2005). Modeling and analyzing power consumption in sensor networks nodes based on differential hybrid Petri nets. Paper presented at the 31st *Annual Conference of IEEE Industrial Electronics Society,* 2005. IECON 2005.

Wan, J., Zhao, B. H., and Qin, H. Y. (2017). Petri net modeling and VHDL implementation of digital systems. *Application Research of Computers*, 34(02), 458-462

Wei, W., Song, H. B., Li, W., Shen, P. Y., and Vasilakos, A. (2017). Gradient-driven parking navigation using a continuous information potential field based on wireless sensor network. *Information Sciences*, 408, 100-114. doi:10.1016/j.ins.2017.04.042

Yang, M., Wang, A. M., Sun, G., and Zhang, Y. (2018). Deploying charging nodes in wireless rechargeable sensor networks based on improved firefly algorithm. *Computers & Electrical Engineering*, 72, 719-731.

Yu, Z. H., Fu, X. A., Cai, Y. L., and Vuran, M. C. (2011). A Reliable Energy-Efficient Multi-Level Routing Algorithm for Wireless Sensor Networks Using Fuzzy Petri Nets. *Sensors,* 11(3), 3381-3400. doi:10.3390/s110303381

Zairi, S., Mezni, A., and Zouari, B. (2015). Formal Approach for Modeling, Verification and Performance Analysis of Wireless Sensors Network. In M. C. AguayoTorres, G. Gomez, & J. Poncela (Eds.), *Wired/Wireless Internet Communications*, Wwic 2015 (Vol. 9071, pp. 381-395). Berlin: Springer-Verlag Berlin.

Zeng, W., and Hong, Z. (2009, 22-24 May 2009). A SPN-Based Performance Evaluation of Wireless Sensor Networks. Paper presented at the 2009 *Second International Symposium on Electronic Commerce and Security.*

Zhang, G. Y., Zhao, W. G., and Yan, X. T. (2017). Collaborative Design Implementation on the PN-PDDP Model for the Complex Coupled Rotor Systems. *Control Engineering and Applied Informatics,* 19(3), 69-78.

Zhang, Q. F., and Li, H. (2007). MOEA/D: A multiobjective evolutionary algorithm based on decomposition. *Ieee Transactions on Evolutionary Computation*, 11(6), 712-731.

Zitzler, E., and Thiele, L. (1999). Multiobjective evolutionary algorithms: A comparative case study and the Strength Pareto approach. *Ieee Transactions on Evolutionary Computation*, 3(4), 257-271.